DOI 10.1002/pmic.201400537 *Proteomics* 2015, *15*, 2342–2349

RESEARCH ARTICLE

Label-free profiling of white adipose tissue of rats exhibiting high or low levels of intrinsic exercise capacity

Kelly Bowden-Davies[1], Joanne Connolly[2], Paul Burghardt[3], Lauren G. Koch[3], Steven L. Britton[3,4] and Jatin G. Burniston[1]

[1] Research Institute for Sport and Exercise Sciences, Liverpool John Moores University, Liverpool, UK
[2] Waters MSHQ, Wilmslow, Manchester, UK
[3] Department of Anaesthesiology, University of Michigan, Ann Arbor, MI, USA
[4] K.G. Jebsen Center for Exercise in Medicine, Department of Circulation and Medical Imaging, Norwegian University of Science and Technology, Trondheim, Norway

Divergent selection has created rat phenotypes of high- and low-capacity runners (HCR and LCR, respectively) that have differences in aerobic capacity and correlated traits such as adiposity. We analyzed visceral adipose tissue of HCR and LCR using label-free high-definition MS (elevated energy) profiling. The running capacity of HCR was ninefold greater than LCR. Proteome profiling encompassed 448 proteins and detected 30 significant ($p < 0.05$; false discovery rate <10%, calculated using q-values) differences. Approximately half of the proteins analyzed were of mitochondrial origin, but there were no significant differences in the abundance of proteins involved in aerobic metabolism. Instead, adipose tissue of LCR rats exhibited greater abundances of proteins associated with adipogenesis (e.g. cathepsin D), ER stress (e.g. 78 kDa glucose response protein), and inflammation (e.g. Ig gamma-2B chain C region). Whereas the abundance antioxidant enzymes such as superoxide dismutase [Cu-Zn] was greater in HCR tissue. Putative adipokines were also detected, in particular protein S100-B, was 431% more abundant in LCR adipose tissue. These findings reveal low running capacity is associated with a pathological profile in visceral adipose tissue proteome despite no detectable differences in mitochondrial protein abundance.

Received: November 16, 2014
Revised: January 29, 2015
Accepted: March 4, 2015

Keywords:
Adipokines / Aerobic capacity / Animal proteomics / Label-free quantitation / Metabolic syndrome / Obesity

Additional supporting information may be found in the online version of this article at the publisher's web-site

1 Introduction

Worldwide the levels of obesity have almost doubled since 1980 and approximately 3.4 million adults die each year as a result of being overweight or obese. In particular, abdominal obesity is associated with a heightened risk of cardiovascular disease and type 2 diabetes mellitus (T2DM) and is a cardinal feature of the metabolic syndrome. Indeed, almost half of the worldwide diabetes burden, and one-quarter of the ischemic heart disease burden is attributable to overweight and obesity.

Diet-induced models of obesity are common as are targeted and spontaneous genetic models such as the Zucker fatty rat [1]. However, in addition to diet and energy intake, physical activity and energy expenditure also impact on whole body energy balance and composition. We have used divergent artificial selection on running capacity to create high-capacity runner (HCR) and low-capacity runner (LCR) rats that have profound differences in running capacity and exhibit numerous correlated traits relevant to human disease. While HCR

Correspondence: Dr. Jatin G. Burniston, Muscle Physiology and Proteomics Laboratory, Research Institute for Sport and Exercise Sciences, Tom Reilly Building, Liverpool John Moores University, Byrom Street, Liverpool, L3 3AF, UK.
E-mail: j.burniston@ljmu.ac.uk
Fax: +44-151-904-6284

Abbreviations: **GeLC-MS/MS**, orthogonal SDS-PAGE and LC-MS/MS; **HCR**, high capacity runner; **HDMS^E**, high-definition mass spectrometry (elevated energy); **LCR**, low-capacity runner

Colour Online: See the article online to view Fig. 1 in colour.

animals are relatively lean and have a low disease risk profile, LCR rats are overweight [2], hypertensive [3], insulin resistant [4], and have a significantly shorter life expectancy [5]. Moreover, in response to a high fat diet, LCR are more prone to exacerbation of this insulin-resistant condition whereas HCR are protected despite their low levels of habitual activity and relatively greater calorific intake [2].

Biochemical assessment of carcass composition [6] reveals the percentage body fat of adult LCR (~36%) is more than double that (~16%) of HCR. More specifically, the greater adiposity of LCR is due to the increased masses of retroperitoneal, omental, and periretroproductive fat pads [7], and enlargement of such visceral adipose depots, in particular, is intimately associated with cardiometabolic disease risk [8]. In striated muscle, the weight of evidence from our HCR/LCR model points to mechanistic links between low respiratory capacity and mitochondrial dysfunction associated with defects in contractile function and substrate metabolism. In contrast, recent examination of visceral adipose tissue of LCR/HCR [9] reported no major differences in mitochondrial enzyme content despite overt differences in running capacity and adipose tissue mass. It seems unlikely artificial selection has left adipose tissue unaffected but as yet the nature of the effect in adipose tissue is unknown at the molecular level.

Herein, we use label-free proteomic profiling as a nontargeted approach to discover differences between HCR and LCR. This approach is designed to highlight candidate biomarkers or direct future research regarding the greater adiposity and enhanced rate of adipogenesis of LCR in response to environmental stresses such as a high-fat diet. We used a quadrupole time-of-flight (Q-TOF) mass spectrometer operated in data-independent acquisition (DIA) mode, which affords more detailed detection of peak profiles and improves measurement precision compared to classic data-dependent acquisitions [10]. Relative expression data generated by this instrument was analyzed using the "Hi-3" method wherein label-free quantitation is performed on the summed ion counts from the three most intense peptides from each protein normalized to an exogenous protein spiked in to each sample [11]. This approach affords robust differential analysis based on the normalized abundance of proteins and was performed on biological replicates of HCR and LCR animals.

2 Materials and methods

2.1 Animal model and tissue collection

The inception of HCR-LCR strains from a founder population of genetically heterogeneous N:NIH rats has been described in detail [12]. Animals were housed (two per cage) in accordance with the University of Michigan Committee guidelines on the use and care of animals. Environmental conditions were 20–21°C, 40–50% relative humidity with a 12-h light (0600–1800) and dark cycle, and food and water were available ad libitum.

Rats from generation 26 of selection were used in the current work. Consistent with our standard selection procedures [12], HCR and LCR animals were phenotyped by their maximum running capacity at 10 weeks of age. Briefly, endurance trials were performed on an inclined (15 degrees) motorized treadmill (Columbus Instruments, OH) on five consecutive days. The treadmill velocity began at 10 m/min and was increased by 1 m/min every 2 min until exhaustion. Exhaustion was operationally defined as the third time a rat could no longer keep pace with the speed of the treadmill and remained on the shock grid for 2 s. At this point, the total distance (m) run was recorded. The single best distance of the five trials was considered as the performance indicator most closely associated with the heritable component of endurance running capacity. Other than the aforementioned phenotyping trials, rats used in the current report were sedentary and did not perform exercise training. Therefore, the difference in running capacity between HCR and LCR is primarily an innate response to selection.

Two weeks after completing the exercise trials male HCR and LCR rats ($n = 6$, of each) were weighed and anesthetized using sodium pentobarbital (60 mg/kg body mass). Retroperitoneal fat pads were surgically excised, then freeze-clamped in liquid nitrogen, and stored at −80°C as part of our routine tissue archiving procedure.

2.2 Sample preparation

Visceral fat samples (~100 mg) were homogenized on ice in ten volumes of 1% (v/v) Triton x-100, 250 mM sucrose, 100 mM NaCl, 5 mM EDTA, 25 mM Tris, pH 7.4, at 4°C, containing complete protease inhibitor (Roche Diagnostics). After centrifugation at 12 000 × *g*, 4°C for 45-min supernatants were decanted and an aliquot containing 100 μg protein precipitated in five volumes of acetone for 1 h at −20°C. Pellets were resuspended in 1% (w/v) SDS and incubated at 90°C for 30 min before being washed twice through 5 kDa molecular weight cut-off spin columns (Vivaspin; Sigma-Aldrich, Gillingham, UK) using 0.1% (w/v) Rapigest SF (Waters; Milford, MA, USA) in 50 mM ammonium bicarbonate (500 μL per wash). Protein suspensions were concentrated to 50 μL, then incubated at 80°C for 15 min. DTT was added (final concentration 1 mM) and incubated at 60°C for 15 min followed by incubation while protected from light in the presence of 5 mM iodoacetamide at 4°C. Sequencing grade trypsin (Promega; Madison, WI, USA) was added at a protein ratio of 1:50 and digestion allowed to proceed at 37°C overnight. Digestion was terminated by the addition of 2 μL concentrated TFA and peptide solutions were cleared by centrifugation at 13 000 × *g* for 5 min. Samples were diluted 1:1 with a tryptic digest of yeast alcohol dehydrogenase (100 fmol/ μL) to

enable the amount of each identified protein to be quantified, as described previously using a "Hi 3" methodology [11].

2.3 High-definition MS (elevated energy)

Tryptic peptide mixtures were analyzed by nanoscale ultra-performance liquid chromatography (nanoACQUITY, Waters) and online nano electrospray ionisation (ESI) ion-mobility mass spectrometry (HDMS^E; SYNAPT G2-S, Waters, Manchester, UK). Samples (200 ng tryptic peptides) were loaded in aqueous 0.1% (v/v) formic acid via a Symmetry C_{18} 5 μm, 5 mm x 300 μm precolumn (Waters). Separation was conducted at 35°C through a HSS T3 C_{18} 3 μm, 15 cm × 75 μm analytical reverse phase column (Waters). Peptides were eluted using a gradient rising to 40% ACN 0.1% (v/v) formic acid over 90 min at a flow rate of 300 nL/min. Additionally, a Lockmass reference (100 fmol/ μL Glu-1-fibrinopeptide B) was delivered to the NanoLockSpray source of the mass spectrometer at a flow rate of 500 nL/ min, and was sampled at 60-s intervals.

For all measurements, the mass spectrometer was operated in a data-independent positive ESI mode at a resolution of >20 000 FWHM. Prior to analysis, the time-of-flight analyzer was calibrated with an NaCsI mixture from *m/z* 50 to 1990. HDMS^E analyses were conducted within the Triwave ion guide. Accumulated ions were separated according to their drift time characteristics in the N_2 gas-filled mobility cell prior to CID alternating between low (4 eV) and elevated (14-40 eV) collision energies at a scan speed of 0.9 s per function over 50–2000 *m/z*.

Each biological sample was analyzed in replicate. Analytical data were LockMass corrected postacquisition using the doubly charged monoisotopic ion of the Glu-1-fibrinopeptide B. Charge reduction and deconvolution of potential parent-fragment correlation was achieved in the first instance by means of retention and drift time alignment, as described previously [13]. Briefly, protein identifications and quantification information were extracted using the dedicated algorithms employed in ProteinLynx GlobalSERVER (PLGS) v2.5 (Waters). Peak lists were searched against the Uniprot database (18 January 2012) restricted to 'Rattus' (7500 entries). The enzyme specificity was trypsin allowing one missed cleavage, carbamidomethyl modification of cysteine (fixed), oxidation of methionine (variable), and the parent and fragment ion ppm error automatically calculated from the data. Decoy databases were employed to allow the calculation of identification error rates and scoring of the database searches was refined by correlation of physicochemical properties of fragmented peptides from theoretical and experimental data. Data were uploaded and checked in PRIDE converter and inspector [14]. Functional enrichment testing was performed using the Database for Annotation, Visualisation and Integrated Discovery (DAVID v6.7; [15, 16]) and protein interactions were investigated using the search tool for interacting genes/proteins (STRING v9.1; [17]).

3 Results

3.1 Exercise capacity of HCR and LCR rats

Proteome profiling was performed on retroperitoneal fat from male HCR and LCR of generation 26. The average running capacity of HCR (1926 ± 160 m) was ~ ninefold greater (p <0.0001) than LCR (216 ± 34 m), whereas the average body weight of LCR (329 ± 23 g) was ~50% greater (p <0.0001) than HCR (242 ± 13 g). Fat pad masses were not recorded during the tissue archiving procedure, but as a point of reference, Table 1 in Demarco *et al.* [7] reports the masses of retroperitoneal, perireproductive, and omental fat depots in male and female HCR and LCR rats from generation 27 at 30 weeks of age. Consistent with a number of earlier studies (e.g. [2, 18–21]), Demarco et al., [7] reports retroperitoneal mass in male LCR (11.14 ± 1.2 g) was more than double (p <0.005) that of HCR (4.2 ± 0.5 g).

3.2 HDMSE analysis of visceral fat proteins

HDMS^E analysis of replicate adipose tissue homogenates from six HCR and six LCR rats produced a nonredundant list of 1023 proteins at a false-positive rate <4%. This number is close to the 1493 proteins identified in Xie *et al.* [22] using LC-MS/MS analysis of 20 molecular weight fractions (i.e. GeLC-MS/MS) of adipocytes isolated from human subcutaneous adipose tissue. Adachi *et al.* [23] reports a more comprehensive catalog (a total of 3287 proteins) of adipocyte proteins, which was achieved by fractionating 3T3-L1 adipocytes to nuclear, mitochondrial, membrane, and cytosolic components followed by GeLC-MS/MS to culminate in a total of 45 fractions per sample. MS data of technical replicates of each HCR and LCR sample are available in the PRoteomics IDEntification (PRIDE) database (www.ebi.ac.uk/pride/). Supporting Information Table 1 reports the identity and relative abundance of a subset of 448 proteins that were replicated in at least four out of the six samples from each group and were used in differential statistical analysis of the HCR and LCR groups. Supporting Information Table 1 also includes data extracted from Adachi *et al.*, [23] reporting homologs of proteins identified in the mouse adipocyte proteome.

Based on the estimated protein abundance on-column, the dynamic range of the current analysis spanned three orders of magnitude. Among the most abundant (amount on column) proteins identified were serum albumin (~75 pg), carbonic anhydrase (~28 pg), and fatty acid ethyl ester synthase (~26 pg), which is a major lipase in white adipose tissue. The least abundant (amount on column) proteins meeting the inclusion criteria for statistical analysis were galectin-5 (0.06 pg), dimethylarginine dimethylaminohydrolase 1 (0.063 pg), and mitochondrial fusion protein 1 (0.076 pg). Supporting Information Table 1 reports the protein scores, number of peptides, sequence coverage, estimated abundance, and

Table 1. Differences in protein abundance between HCR and LCR visceral adipose tissue

Description	Database ID	Estimated protein abundance (pg)		Percentage difference	*p* value
		HCR	LCR		
Adipogenesis/adipocyte differentiation					
Protein S100-B	P04631	0.37 ± 0.28	1.71 ± 0.57	+ 431%	0.0001
Cathepsin D	P24268	0.50 ± 0.09	0.93 ± 0.21	+ 88%	0.0010
Carbonic anhydrase 1	B0BNN3	1.42 ± 0.37	2.05 ± 0.52	+ 44%	0.0025
Glycerol-3-phosphate dehydrogenase [NAD+], cytosolic	O35077	6.42 ± 1.34	9.03 ± 0.98	+ 41%	0.0000
Aldehyde dehydrogenase, mitochondrial	P11884	5.71 ± 0.56	6.87 ± 1.20	+ 20%	0.0054
Long chain fatty acid CoA-ligase 1	P18163	14.07 ± 1.25	16.65 ± 0.92	+ 18%	0.0002
Sulfotransferase 1A1	P17988	0.31 ± 0.06	0.15 ± 0.06	−89%	0.0003
Galectin-1	P11762	7.92 ± 0.64	6.91 ± 0.92	−15%	0.0049
Antioxidant/stress response					
Mitogen-activated protein kinase 3	P21708	0.23 ± 0.06	0.35 ± 0.08	+43%	0.0047
78 kDa glucose-regulated protein	P06761	4.16 ± 0.35	4.90 ± 0.53	+18%	0.0017
Heat shock protein beta-1	P42930	2.70 ± 0.42	1.82 ± 0.20	−48%	0.0000
Glutathione S-transferase P	P04906	2.14 ± 0.42	1.51 ± 0.25	−42%	0.0002
Peroxiredoxin-6	O35244	1.65 ± 0.42	1.20 ± 0.25	−38%	0.0053
Superoxide dismutase [Cu-Zn]	P07632	2.92 ± 0.45	1.20 ± 0.25	−30%	0.0003
Selenium-binding protein 1	Q8VIF7	2.90 ± 0.28	2.23 ± 0.17	−23%	0.0003
Immune cell function					
Ig gamma-2B chain C region	P20761	0.19 ± 0.08	0.89 ± 0.38	+ 362%	0.0005
Ig kappa chain C region, B allele	P01835	1.24 ± 0.51	2.60 ± 0.93	+110%	0.0044
Class I histocompatability antigen, Non-RT1.A alpha	P15978	0.20 ± 0.08	0.32 ± 0.05	+62%	0.0023
Ig gamma-2A chain C region	P20760	3.15 ± 0.90	4.91 ± 1.72	+56%	0.0039
Energy metabolism					
Triosephosphate isomerase	P48500	2.45 ± 0.35	3.16 ± 0.66	+29%	0.0049
Glyceraldehyde-3-phosphate dehydrogenase	P04797	4.46 ± 0.55	5.28 ± 0.76	+18%	0.0058
Phosphoglycerate kinase	P16617	2.63 ± 0.21	2.06 ± 0.27	−27%	0.0000
ADP/ATP translocase 1	Q05962	0.62 ± 0.05	0.48 ± 0.04	−28%	0.0021
Miscellaneous					
T-kininogen 2	P08932	0.26 ± 0.03	0.38 ± 0.10	+47%	0.0070
Hemopexin	P20059	7.34 ± 1.22	10.14 ± 0.95	+38%	0.0000
Serotransferrin	P12346	26.24 ± 2.41	31.0 ± 3.37	+18%	0.0015
Ras-related protein Rab-11A	P62494	0.40 ± 0.06	0.29 ± 0.04	−35%	0.0068
Purine nucleoside phosphorylase	P85973	1.12 ± 0.09	0.83 ± 0.19	−34%	0.0003
Annexin A3	P14669	1.97 ± 0.27	1.60 ± 0.23	−23%	0.0028
Profilin-1	P62963	2.60 ± 0.35	2.19 ± 0.16	−18%	0.0026

Proteins under each subheading are ranked (greatest first) by relative differences (percentage difference) in LCR compared to HCR. Each of the listed proteins exhibited significant ($p<0.05$) differences in abundance at an FDR of <10%. Description and database ID relate to the protein name and accession number identified from HDMSE searches of the UniProt Rattus database performed in ProteinLynx Global Server. Protein abundance (pg) on column was estimated relative to a 'spiked' yeast alcohol dehydrogenase digest.

differences in relative abundance between HCR and LCR for the 448 proteins included in the statistical analysis.

Gene ontology analysis performed using DAVID found the majority of proteins were of cytosolic (130 proteins) or mitochondrial (128 proteins) origin. Prominent Biological Processes included: alcohol catabolic process (30 proteins) and glucose catabolic process (27 proteins). While the main molecular functions related to GTP binding (50 proteins) and nucleotide binding (172 proteins). When clustered according to associations in the Kyoto Encyclopaedia of Genes and Genomes (KEGG; http://www.genome.jp/kegg/), the top ranking pathway was Glycolysis/gluconeogensis, which encompassed 27 proteins representing 6.2% of the documented pathway. Other prominent pathways included fatty acid metabolism (18 proteins) and glutathione metabolism (19 proteins).

A total of 79 statistically significant ($p<0.05$) differences in protein abundance were detected between HCR and LCR adipose samples and after correction (q-value) for multiple testing, 30 significant differences exhibited a false discovery rate of less than 10% ($q<0.1$). Table 1 reports the protein identity and differences in abundance between HCR and LCR for

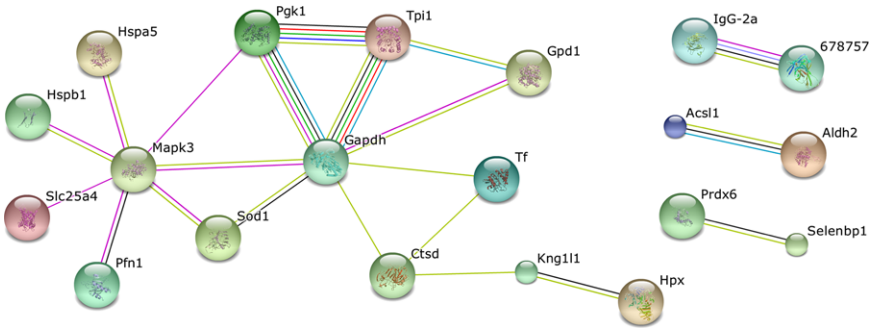

Figure 1. Association network drawn from proteins that differed in abundance in HCR and LCR visceral adipose tissue. Proteins that exhibited statistically significant ($p<0.05$, FDR <10%) differences in abundance (Table 1) were imported to the statistical tool for the retrieval of interacting genes/proteins (STRING). Nodes represent individual proteins annotated with common gene names: 678 757, Ig kappa chain C region, B allele; Acsl1, long-chain fatty acid Co-A ligase 1; Aldh2, aldehyde dehydrogenase 2; Ctsd, cathepsin D; Gapdh, glyceraldehyde-3-phosphate dehydrogenase; Gpd1, glycerol-3-phosphate dehydrogenase [NAD+] cytosolic; Hpx, Hemopexin; Hspa5, 78-kDa glucose-regulated protein; Hspb1, heat shock protein beta-1; IgG-2a, Ig gamma-2B Chain C region; Kng1|1, T-kininogen 2; Mapk3, mitogen-activate protein kinase 3; Pfn1, profilin-1; Pgk1, phosphoglycerate kinase; Prdx6, peroxiredoxin-6; Selenbp1, selenium binding protein-1; Slc25a4, ADP/ATP translocase 1; Sod1, superoxide dismutase [Cu-Zn]; Tf, serotransferrin; Tpi1, triosephosphate isomerase. Vectors between nodes are color coded to represent different levels of information, including: evidence of co-expression (black), protein–protein interaction (pink), concurrence in databases such as the Kyoto Encyclopaedia of Genes and Genomes (KEGG; blue) or PubMed abstracts (green). A medium confidence cut-off was used and no additional interactions were added.

the top-ranked ($p<0.05$, FDR <10%) 30 proteins. A number of the proteins that differed between HCR and LCR have previously been associated with adipogenesis or adipocyte differentiation in vitro. Proteins associated with antioxidant or cellular stress response, immune cell function, and energy metabolism were other prominent features. Among the most abundant of the differentially expressed proteins were serotransferrin (~29 pg on column) and long-chain fatty acid CoA-ligase 1 (~15 pg on column) while the least abundant (>0.5 pg on column) differentially expressed proteins detected included sulfotransferase 1A1, IgG2B C-chain, and mitogen-activated protein kinase 3.

The search tool for the retrieval of interacting genes/proteins (STRING) was used to construct a graphical network (Fig. 1) based on evidence of co-expression, protein–protein interaction, co-occurrence in KEGG pathways, and literature mining. The network constructed from 15 proteins that matched to the STRING DB and were significantly ($p<0.05$, FDR <10%) more abundant in LCR included protein–protein interactions between Mapk3 and Hspa5, Aldh2, TF, Acsl1, Tpi1, and Gapdh. Protein–protein interactions were also found between Aldh2 and Tpi1, and for Acsl1 and Hspa5. Co-expression was reported between Tf and Hpx, Tpi1 and Gapdh, Acsl1 and Ctsd, Mapk3 and Ctsd, Igg-2a and 678757 (IgG-2B chain C region). In addition, links were drawn based on co-occurrence in KEGG pathways and text mining.

Fewer interactions were found within the 13 proteins that were significantly ($p<0.05$, FDR <10%) more abundant in HCR. The only notable evidence being co-expression of peroxiredoxin 6 and selenium-binding protein in one proteomic profiling experiment.

4 Discussion

Despite a ninefold difference in innate running capacity, there was no difference in the abundance of mitochondrial proteins between HCR and LCR visceral adipose tissue. Instead, our nontargeted analysis highlighted significant differences in putative adipokines and proteins involved in adipogenesis, oxidative stress, and inflammation. Our label-free profiling encompassed 448 proteins and detected 30 statistically significant ($p<0.05$, FDR <10%) differences in protein abundance. The majority of these proteins have previously been detected in proteomic analyses of adipocytes isolated from human [22] or mouse [23] adipose tissues. Notable exceptions include IgG and MHC proteins that were significantly more abundant in LCR. This may indicate greater infiltration of inflammatory cells in LCR visceral adipose tissue.

The role of macrophages and T lymphocytes in adipose tissue inflammation has long been recognized, whereas the role of B lymphocytes has more recently come to light. Herein we report the pro-inflammatory IgG-2B Chain C isotope, which is produced by B cells was 362% more abundant in LCR visceral adipose tissue. The accumulation of B cells in adipose tissue is an early event in diet-induced obesity that precedes T-cell infiltration, the onset of insulin resistance, and macrophage accumulation [24]. During obesity, B cells within adipose tissue may instigate inflammation both by presenting antigen via MHC I to activate CD8+ (i.e. cytotoxic) T cells and through the production of pro-inflammatory IgG2c [25]. When studied in vitro, B cells modulate T-cell release of pro-inflammatory cytokines [26] and our data suggest low aerobic capacity may also be associated with similar pro-inflammatory interactions.

ER stress associated with adipocyte enlargement is another early mechanism associated with inflammatory responses such as the production of TNF-α and infiltration of macrophages to adipose tissue [27]. The 78 kDa glucose-regulated protein (GRP-78, also known as BiP) was more abundant in LCR and is a recognized marker of ER stress that is induced by the unfolded protein response associated with adipogenesis [28] and pharmacological agents such as tunicamycin [29]. ER stress can occur due to the accumulation of unfolded proteins caused by oxidative stress-related protein damage. Accordingly, antioxidant enzymes, including superoxide dismutase, peroxiredoxin 6, and glutathione S-transferase were significantly less abundant in LCR. This finding is consistent with the greater oxidative stress reported in the kidneys [30], liver [21], skeletal muscle [31], and heart [32] of LCR rats and further highlights oxidative stress as a common process associated with low aerobic capacity. Herein nontargeted proteomics also detected a significantly greater (43%) abundance of mitogen-activated protein kinase 3 (ERK1), which is commonly activated in adipocytes exposed to pharmacologically induced ER stress [33] or inflammatory cytokines [34]. This finding adds weight to the hypothesis that low innate aerobic capacity per se is sufficient to predispose animals to obesity and adipose tissue inflammation.

Adipose tissue is recognized as an endocrine organ that secretes adipokines that affect tissues such as the hypothalamus, liver, and skeletal muscle. In addition to well-described adipokines, such as leptin, proteomic studies (e.g. [35–37]) point to a broad array of putative adipokines that may be released or secreted from adipocytes in vitro. In addition, comprehensive mining of the 3T3-L1 adipocyte proteome by Adachi *et al*. [23] highlighted 554 adipocyte proteins with signal peptides for the ER-Gologi export pathway. Five of the proteins that differed in abundance between HCR and LCR (Table 1) either have a signal peptide or have been reported as secreted from adipocytes in vitro. Putative adipokines that were more abundant in LCR visceral adipose tissue include S100-B, cathepsin D, serotransferrin, and GRP-78/ BiP, whereas sulfotransferase 1A1 and galectin-1 were more abundant in HCR. The majority of the above proteins have been associated with obesity, metabolic syndrome, or type 2 diabetes. For example, mRNA expression of cathepsin D is upregulated in adipose tissue of mice exposed to a high-fat diet and in obese humans, and studies in vitro suggest differentiation of pre-adipocytes is dependent upon cathepsin D expression [38]. Sulfotransferase 1A1 does not have a signal peptide for the golgi excretory pathway but has previously been highlighted as a gene associated with T2DM by genome-wide scans. Indeed, sulfotransferase 1A1 mRNA expression is downregulated in response to HFD alongside other candidates close to genetic loci for obesity [39]. Galectin-1 also lacks a signal peptide but is reported to be more abundant in plasma of T2DM patients, which contrasts with our findings. However, galectin-1 is highly expressed in skeletal muscle [40] and exposure of skeletal muscle to glucose increases galectin-1 [41]. Thus, the elevations in plasma galectin-1 in T2DM patients may primarily arise from skeletal muscle rather than adipose tissue.

S100-B does not have a canonical signal peptide but is relatively abundant in adipose tissue (HCR 0.37 ± 0.28; LCR 1.7 ± 0.57 pg on column) and is widely documented as a secreted protein. Circulating levels of S100-B correlate positively with BMI [42] and visceral obesity [43] but this is not evident in all studies (e.g [44]) and because S100-B is also released from brain astrocytes it is also regarded as a biomarker of blood–brain barrier permeability. Nonetheless, the current finding that an estimated 100% difference in adipose tissue mass is associated with a >400% increase in S100-B abundance supports the role of this protein as a sensitive biomarker of adiposity. Furthermore, S100-B has recently been implicated mechanistically in the interaction between adipocytes and macrophages in vitro. Fujiya et al. [45] report S100-B stimulates the release of TNF-α from RAW macrophages and primary monocytes, and upregulates markers of M1 macrophages. Correspondingly, TNF-α augments S100-B secretion from 3T3-L1 adipocytes creating a reciprocal interaction that may amplify the inflammatory response of adipose tissues in obese subjects.

When fed a high-fat diet (HFD), LCR gain significantly more weight than HCR despite the fact that HCR consume a greater amount of calories relative to body mass [2] In the current work, many of the proteins that were more abundant in LCR visceral adipose tissue are also recognized markers of adipocyte differentiation. For example, the greater abundances of glycerol-3-phosphate dehydrogenase and long-chain fatty acid CoA ligase may contribute to the relatively greater propensity for obesity in LCR rats. Our nontargeted analysis was able to detect important adipose tissue proteins highlighted through hypothesis-led research, including lipoprotein lipase, fatty acid translocase, adipose fatty acid binding protein, adipose triglyceride lipase, hormone-sensitive lipase, fatty acid synthase, perilipin 1 and retinol binding protein 4. However, the abundances of these proteins were not significantly different between HCR and LCR visceral adipose tissue. Interestingly, LCR did exhibit lesser abundance ($p<0.05$, FDR >10%) of comparative gene identification-58, which enhances the lipase activity of adipose triglyceride lipase [46] and has previously been reported to be less abundant in LCR adipose tissue [9].

While adiposity is a correlated trait of selection on running capacity, it is not associated with overt differences in the profile of enzymes of aerobic metabolism in adipose tissue. Instead, our nontargeted proteomic analysis has revealed LCR visceral adipose tissue has relatively poor defences against oxidative stress and exhibits markers of adipocyte differentiation, ER stress, and inflammation. Moreover, several putative adipokines differed in abundance between HCR and LCR. In particular S100-B protein, which has recently been mechanistically linked in adipose tissue inflammation was 431% more abundant in LCR and may represent candidate biomarker of clinical relevance.

The LCR-HCR rat model system was funded by the Office of Research Infrastructure Programs/OD grant R24OD010950 and by grant R01DK099034 (to L.G.K. and S.L.B.) from the National Institutes of Health. S.L.B. was also supported by National Institutes of Health grants R01DK077200, and R01GM104194. We acknowledge the expert care of the rat colony provided by Molly Kalahar and Lori Heckenkamp. Contact L.G.K. (lgkoch@med.umich.edu) or S.L.B. (brittons@umich.edu) for information on the LCR and HCR rats: these rat models are maintained as an international resource with support from the Department of Anaesthesiology at the University of Michigan, Ann Arbor, MI, USA.

5 References

[1] Zucker, L. M., Zucker, T. F., Fatty, a new mutation in the rat. *J. Hered.* 1961, *52*, 275–278.

[2] Noland, R. C., Thyfault, J. P., Henes, S. T., Whitfield, B. R. et al., Artificial selection for high-capacity endurance running is protective against high-fat diet-induced insulin resistance. *Am. J. Physiol. Endocrinol. Metab.* 2007, *293*, E31–E41.

[3] Wisloff, U., Najjar, S. M., Ellingsen, O., Haram, P. M. et al., Cardiovascular risk factors emerge after artificial selection for low aerobic capacity. *Science* 2005, *307*, 418–420.

[4] Rivas, D. A., Lessard, S. J., Saito, M., Friedhuber, A. M. et al., Low intrinsic running capacity is associated with reduced skeletal muscle substrate oxidation and lower mitochondrial content in white skeletal muscle. *Am. J. Physiol. Regul. Integr. Comp. Physiol.* 2011, *300*, R835–R843.

[5] Koch, L. G., Kemi, O. J., Qi, N., Leng, S. X., et al., Intrinsic aerobic capacity sets a divide for aging and longevity. *Circ. Res.* 2011, *109*, 1162–1172.

[6] Novak, C. M., Escande, C., Burghardt, P. R., Zhang, M., et al., Spontaneous activity, economy of activity, and resistance to diet-induced obesity in rats bred for high intrinsic aerobic capacity. *Horm. Behav.* 2010, *58*, 355–367.

[7] Demarco, V. G., Johnson, M. S., Ma, L., Pulakat, L., et al., Overweight female rats selectively bred for low aerobic capacity exhibit increased myocardial fibrosis and diastolic dysfunction. *Am. J. Physiol. Heart Circ. Physiol.* 2012, *302*, H1667–H1682.

[8] Després, J. P., Lemieux, I., Bergeron, J., Pibarot, P., et al., Abdominal obesity and the metabolic syndrome: contribution to global cardiometabolic risk. *Arterioscler. Thromb. Vasc. Biol.* 2008, *28*, 1039–1049.

[9] Stephenson, E. J., Lessard, S. J., Rivas, D. A., Watt, M. J. et al., Exercise training enhances white adipose tissue metabolism in rats selectively bred for low- or high-endurance running capacity. *Am. J. Physiol. Endocrinol. Metab.* 2013, *305*, E429–E438.

[10] Levin, Y., Hradetzky, E., Bahn, S., Quantification of proteins using data-independent analysis (MSE) in simple andcomplex samples: a systematic evaluation. *Proteomics* 2011, *11*, 3273–3287.

[11] Silva, J. C., Gorenstein, M. V., Li, G. Z., Vissers, J. P., Geromanos, S. J., Absolute quantification of proteins by LCMSE: a virtue of parallel MS acquisition. *Mol. Cell Proteomics.* 2006, *5*, 144–156.

[12] Koch, L. G., Britton, S. L., Artificial selection for intrinsic aerobic endurance running capacity in rats. *Physiol. Genomics* 2001, *5*, 45–52.

[13] Li, G. Z., Vissers, J. P., Silva, J. C., Golick, D. et al., Database searching and accounting of multiplexed precursor and product ion spectra from the data independent analysis of simple and complex peptide mixtures. *Proteomics* 2009, *9*, 1696–1719.

[14] Csordas, A., Ovelleiro, D., Wang, R., Foster, J. M., et al., PRIDE: quality control in a proteomics data repository. *Database (Oxford)* 2012, *2012*, bas004.

[15] Huang, d. a. W., Sherman, B. T., Lempicki, R. A., Systematic and integrative analysis of large gene lists using DAVID bioinformatics resources. *Nat. Protoc.* 2009, *4*, 44–57.

[16] Huang, d. a. W., Sherman, B. T., Lempicki, R. A., Bioinformatics enrichment tools: paths toward the comprehensive functional analysis of large gene lists. *Nucleic Acids Res.* 2009, *37*, 1–13.

[17] Franceschini, A., Szklarczyk, D., Frankild, S., Kuhn, M. et al., STRING v9.1: protein-protein interaction networks, with increased coverage and integration. *Nucleic Acids Res.* 2013, *41*, D808–D815.

[18] Bowman, T. A., Ramakrishnan, S. K., Kaw, M., Lee, S. J. et al., Caloric restriction reverses hepatic insulin resistance and steatosis in rats with low aerobic capacity. *Endocrinology* 2010, *151*, 5157–5164.

[19] Lessard, S. J., Rivas, D. A., Stephenson, E. J., Yaspelkis, B. B. et al., Exercise training reverses impaired skeletal muscle metabolism induced by artificial selection for low aerobic capacity. *Am. J. Physiol. Regul. Integr. Comp. Physiol.* 2010, *300*, R175–R182.

[20] Naples, S. P., Borengasser, S. J., Rector, R. S., Uptergrove, G. M. et al., Skeletal muscle mitochondrial and metabolic responses to a high-fat diet in female rats bred for high and low aerobic capacity. *Appl. Physiol. Nutr. Metab.* 2010, *35*, 151–162.

[21] Thyfault, J. P., Rector, R. S., Uptergrove, G. M., Borengasser, S. J. et al., Rats selectively bred for low aerobic capacity have reduced hepatic mitochondrial oxidative capacity and susceptibility to hepatic steatosis and injury. *J. Physiol.* 2009, *587*, 1805–1816.

[22] Xie, X., Yi, Z., Bowen, B., Wolf, C. et al., Characterization of the human adipocyte proteome and reproducibility of protein abundance by one-dimensional gel electrophoresis and HPLC-ESI-MS/MS. *J. Proteome Res.* 2010, *9*, 4521–4534.

[23] Adachi, J., Kumar, C., Zhang, Y., Mann, M., In-depth analysis of the adipocyte proteome by mass spectrometry and bioinformatics. *Mol. Cell Proteomics* 2007, *6*, 1257–1273.

[24] Duffaut, C., Galitzky, J., Lafontan, M., Bouloumié, A., Unexpected trafficking of immune cells within the adipose tissue during the onset of obesity. *Biochem. Biophys. Res. Commun.* 2009, *384*, 482–485.

[25] Winer, D. A., Winer, S., Shen, L., Wadia, P. P. et al., B cells promote insulin resistance through modulation of T cells and

production of pathogenic IgG antibodies. *Nat. Med.* 2011, *17*, 610–617.

[26] DeFuria, J., Belkina, A. C., Jagannathan-Bogdan, M., Snyder-Cappione, J. et al., B cells promote inflammation in obesity and type 2 diabetes through regulation of T-cell function and an inflammatory cytokine profile. *Proc. Natl. Acad. Sci. USA* 2013, *110*, 5133–5138.

[27] Gustafson, B., Hammarstedt, A., Andersson, C. X., Smith, U., Inflamed adipose tissue: a culprit underlying the metabolic syndrome and atherosclerosis. *Arterioscler. Thromb. Vasc. Biol.* 2007, *27*, 2276–2283.

[28] Basseri, S., Lhoták, S., Sharma, A. M., Austin, R. C., The chemical chaperone 4-phenylbutyrate inhibits adipogenesis by modulating the unfolded protein response. *J. Lipid Res.* 2009, *50*, 2486–2501.

[29] Bull, V. H., Thiede, B., Proteome analysis of tunicamycin-induced ER stress. *Electrophoresis* 2012, *33*, 1814–1823.

[30] Morris, E. M., Whaley-Connell, A. T., Thyfault, J. P., Britton, S. L. et al., Low aerobic capacity and high-fat diet contribute to oxidative stress and IRS-1 degradation in the kidney. *Am. J. Nephrol.* 2009, *30*, 112–119.

[31] Tweedie, C., Romestaing, C., Burelle, Y., Safdar, A. et al., Lower oxidative DNA damage despite greater ros production in muscles from rats selectively bred for high running capacity. *Am. J. Physiol. Regul. Integr. Comp. Physiol.* 2010, *300*, R544–R553.

[32] Burniston, J. G., Kenyani, J., Wastling, J. M., Burant, C. F. et al., Proteomic analysis reveals perturbed energy metabolism and elevated oxidative stress in hearts of rats with inborn low aerobic capacity. *Proteomics* 2011, *11*, 3369–3379.

[33] Deng, J., Liu, S., Zou, L., Xu, C. et al., Lipolysis response to endoplasmic reticulum stress in adipose cells. *J. Biol. Chem.* 2012, *287*, 6240–6249.

[34] Jager, J., Grémeaux, T., Gonzalez, T., Bonnafous, S. et al., Tpl2 kinase is upregulated in adipose tissue in obesity and may mediate interleukin-1beta and tumor necrosis factor-{alpha} effects on extracellular signal-regulated kinase activation and lipolysis. *Diabetes* 2010, *59*, 61–70.

[35] Lehr, S., Hartwig, S., Lamers, D., Famulla, S. et al., Identification and validation of novel adipokines released from primary human adipocytes. *Mol. Cell Proteomics* 2012, *11*, M111.010504.

[36] Rosenow, A., Arrey, T. N., Bouwman, F. G., Noben, J. P. et al., Identification of novel human adipocyte secreted proteins by using SGBS cells. *J. Proteome Res.* 2010, *9*, 5389–5401.

[37] Roca-Rivada, A., Alonso, J., Al-Massadi, O., Castelao, C. et al., Secretome analysis of rat adipose tissues shows location-specific roles for each depot type. *J. Proteomics.* 2011, *74*, 1068–1079.

[38] Masson, O., Prébois, C., Derocq, D., Meulle, A. et al., Cathepsin-D, a key protease in breast cancer, is up-regulated in obese mouse and human adipose tissue, and controls adipogenesis. *PLoS One* 2011, *6*, e16452.

[39] Gutierrez-Aguilar, R., Kim, D. H., Woods, S. C., Seeley, R. J., Expression of new loci associated with obesity in diet-induced obese rats: from genetics to physiology. *Obesity (Silver Spring).* 2012, *20*, 306–312.

[40] Svensson, A., Tågerud, S., Galectin-1 expression in innervated and denervated skeletal muscle. *Cell Mol. Biol. Lett.* 2009, *14*, 128–138.

[41] Liu, X., Feng, Q., Chen, Y., Zuo, J. et al., Proteomics-based identification of differentially-expressed proteins including galectin-1 in the blood plasma of type 2 diabetic patients. *J. Proteome Res.* 2009, *8*, 1255–1262.

[42] Steiner, J., Schiltz, K., Walter, M., Wunderlich, M. T. et al., S100B serum levels are closely correlated with body mass index: an important caveat in neuropsychiatric research. *Psychoneuroendocrinology* 2010, *35*, 321–324.

[43] Steiner, J., Myint, A. M., Schiltz, K., Westphal, S. et al., S100B serum levels in schizophrenia are presumably related to visceral obesity and insulin resistance. *Cardiovasc. Psychiatry Neurol.* 2010, *2010*, 480707.

[44] Pham, N. A. F., Cucullo, V. A., Teng, L. A., Biberthaler, Q. A. et al., Extracranial sources of S100B do not affect serum levels. *PLoS One* 2010, *5*, e12691.

[45] Fujiya, A., Nagasaki, H., Seino, Y., Okawa, T. et al., The role of S100B in the interaction between adipocytes and macrophages. *Obesity (Silver Spring)* 2014, *22*, 371–379.

[46] Lass, A., Zimmermann, R., Haemmerle, G., Riederer, M. et al., Adipose triglyceride lipase-mediated lipolysis of cellular fat stores is activated by CGI-58 and defective in Chanarin-Dorfman Syndrome. *Cell Metab.* 2006, *3*, 309–319.

